

Semi-Annual Reports 1, 2, 3.

(April 1967)

NORMAL AND STIMULATED RAMAN SPECTROSCOPY

B.P. Stoicheff  
University of Toronto  
Department of Physics

AD 654725

460  
105

Order No. NR 015-813/4-14-65

Contract No. Monr-5012(00)

Code No. 5730K21

Expiration Date 31 May 1967

Contractor The Governors  
University of Toronto

Project Scientist Prof. B.P. Stoichef

Business (416) 928-2946

Home (416) 225-6421

Date of Contract 1 June 1965

Amount of Contract \$36,810.00

JUL 18 1967

Reproduction in whole or in part is permitted for any purpose  
of the United States Government.

This document  
for public  
distribution

RECEIVED

JUL 21 1967

CFSTI

34

A.K. McQuillan and B.P. Stoicheff

## A. Introduction

The angular distribution of anti-Stokes emission in the stimulated Raman processes was discussed in some of the first papers on the theory of the process (Garmire, Panderese and Townes<sup>1</sup>, 1963; Bloembergen and Shen<sup>2</sup>, 1964; Maker and Terhune<sup>3</sup>, 1965). From the momentum-matching condition based on a plane-wave model, maxima of anti-Stokes radiation and minima of Stokes radiation are predicted according to the following wave vector relations:

$$\vec{k}_0 + \vec{k}_{n-1} = \vec{k}_{-1} + \vec{k}_n \quad \vec{k}_0 + \vec{k}_{-1} = \vec{k}_{n-1} + \vec{k}_{-n} \quad (1)$$

Here  $\vec{k}_0$ ,  $\vec{k}_{-1}$ ,  $\vec{k}_n$  and  $\vec{k}_{-n}$  are, respectively, the laser, the first Stokes and the  $n$ th-order anti-Stokes and Stokes wave vectors. Such Raman radiation first observed in calcite<sup>4</sup> (Chiao and Stoicheff, 1964) is called Class I radiation. Agreement between the observed and calculated cone angles was within the experimental error of a few percent, under conditions where essentially a parallel laser beam was incident on the calcite. However there was a significant increase in angle as the focal length of the lens used to focus the laser beam was decreased.

The angular dependence of stimulated emission from many different liquids has been reported. Usually, the cone angles are up to 30 percent larger than the predicted values given by Eq. (1) and such distribution is called Class II. Recent

Garmire<sup>5</sup> has observed Class I radiation in liquids under the condition where feedback (by a tilted reflector to enhance the off-axis Stokes intensity) is present.

Since calcite is the only solid for which the angular dependence has been investigated it seemed worthwhile to pursue such studies with other solids. Diamond was chosen since it exhibits a low threshold for stimulated Raman emission (Eckhardt, Bortfield and Geller<sup>6</sup> 1963). Its spectrum was photographed. The angular dependence of anti-Stokes and Stokes radiation with incident parallel light was measured and a detailed study was made of the changes in cone angles with different beam apertures and different beam convergence.

#### B. Spectrum

The stimulated Raman spectrum of diamond was excited by a giant pulse ruby laser at powers of approximately 1 Mw at  $\lambda$  6943. Single shot photographs were obtained using a grating instrument with dispersion of  $20 \text{ cm}^{-1}/\text{mm}$ . Spectra of the first and second-order Stokes and of the first three orders of anti-Stokes radiation were photographed. These were all observed to be extremely sharp lines and could be accurately measured. The frequency shifts from the exciting line were found to be exact multiples of the fundamental C-C vibrational frequency of  $1331.8 \pm 10 \text{ cm}^{-1}$ .

#### C. Cone Angles with Parallel Exciting Radiation

The experimental arrangement was essentially the same as that described by Chiao and Stoicheff<sup>4</sup>. Emission cones of the first three orders of anti-Stokes and the second-order Stokes radiation

were observed along with the corresponding intensity minima in the diffuse first-order Stokes emission, all in the forward direction. Typical photographs of the intensity maxima and minima are shown in Fig. 1. The measured values of the cone angles are given in Table I and for comparison the values calculated from Eq. (1) are included. It is seen that the agreement is very good for all of the emission angles observed, although not as good for the Stokes minima which were difficult to measure. We conclude that just as for calcite, the theory of the plane-wave phase matching conditions is applicable to diamond.

In order that this theory hold, first-order Stokes radiation must be present at the necessary small angles. This is certainly borne out by the Stokes photograph in Fig. 1 and must originate in scattering within the crystal itself or at its surfaces. There is further confirmation of appreciable feedback of scattered light in the crystal, from the observation of fine structure in the anti-Stokes "rings" which can be explained by multiple beam interference.

The cone angles are found to be independent of incident laser power up to incident power densities three times the threshold value. However, the cone angles are very sensitively dependent on the angle of convergence of the incident laser beam even at threshold, as discussed below. (These results are not in agreement with the early theory of Bloembergen and Shen<sup>2</sup> (1964)).

#### D. Cone Angles with Convergent Exciting Radiation

In this series of experiments the laser radiation was

focussed by lenses of different focal lengths and their incident on the diamond crystal. Focal lengths of 2.7, 3.0, 5.2, 9.8, 17.4, 26.0, 31.0 and 50.0 cm were used and, as before, photographs of the first and second order anti-Stokes "rings" and of the second order Stokes "rings" were obtained. The corresponding angles are plotted against  $1/\text{focal length}$  in Fig. 2 and Fig. 3. A linear relation is evident for the anti-Stokes cone angles with the angles increasing as the focal length becomes shorter. Thus  $\theta_{AS} \propto 1/F$ . However, the second-order Stokes cone angles show a completely different dependence on focal length. The angle decreases sharply with shorter focal lengths and reaches a limiting value of about 0.065 radian.

In another series of experiments the dependence of the cone angles on the aperture of the incident radiation was investigated. A lens with  $f = 5.15$  cm was used to focus the laser beam, apertures of 1.0, 1.6, 1.9, 2.4, 2.8 and 3.6 mm diameter were placed in turn at the centre of the lens and photographs of the rings were obtained. The results are shown in a graph of anti-Stokes cone angle versus aperture diameter, in Fig. 4. The measurements clearly indicate a linear relation  $\theta_{AS} \propto d$ .

These two series of experiments establish the result that the cone angles of anti-Stokes emission depend on the angle of convergence of the incident exciting radiation. More precisely, the change in angle

$$\Delta\theta_{AS} = k a/f$$

where  $k$  is a constant,  $a$  the aperture radius and  $f$  the focal length. The numerical value of  $k$  is  $0.9 \pm 0.2$  or 1.0 within the experimental

accuracy. Thus  $\Delta\theta_{AS} = a/f$  and the first anti-Stokes cone angles are given by

$$\theta_{AS} = 0.053 + a/f$$

where  $a/f$  defines the extremity of the converging laser beam. This result implies that the wave vector relations of Eq. (1) are simply rotated by the angle  $a/f$  as shown in Fig. 5(a).

#### E. Discussion

According to the theory of the stimulated Raman process, anti-Stokes radiation is generated by terms such as  $X_a |E_o|^2 |E_s|$  where  $X_a$  is the susceptibility at  $\omega_o + \omega_r$  and  $E_o$  and  $E_s$  are the electric fields at  $\omega_o$  and  $\omega_o - \omega_r$ . The direction of maximum intensity will thus be governed by the direction of maximum intensity of laser and Stokes radiation. Once these directions have been established, the anti-Stokes cone angle can be determined from the momentum matching condition Eq. (1).

All of our observations can be explained in this way provided that first-order Stokes radiation is predominantly in the forward direction. This condition was satisfied in our experiments. The diamond crystal is in the form of a thin plate, 2.2 mm thick with polished and almost parallel faces. The plate was set with faces at right angles to the beam axis so that when either parallel or convergent laser light was incident on the crystal Stokes radiation along the beam axis was favoured. In fact, because of the high refractive index of diamond ( $\sim 2.4$ ) the plate itself acts as a resonator for the Stokes radiation on

the beam axis. Thus the Stokes intensity is a maximum on axis and falls off in a Gaussian distribution with angle off the axis.

When laser and Stokes radiation interact to produce anti-Stokes emission, that direction will be preferred which makes use of Stokes radiation closest to the axis. With a converging laser beam this means that the laser radiation making the largest angle will be most efficient in production of anti-Stokes radiation. Thus it would appear that only the radiation on the outer extremity of the laser beam, making an angle  $a/f$  would be effective. That is, the wave vector diagram would be rotated as shown in Fig. 5a. An extreme case would occur with laser radiation at the angle  $0.053 + 0.064$  (see Table I) that is at approximately 0.12 rad and with the Stokes radiation on axis.

To test this conclusion, experiments were performed with laser radiation converging at angles 2.5 and 3.1 times the largest angles represented by the results of Figs. 3 and 4. These angles correspond to  $a/f = 0.091$  and  $0.112$  respectively. With a convergence angle of  $0.091$  rad the first anti-Stokes ring was very broad, with a cone angle of  $0.12 \pm 0.02$  rad. With a convergence angle of  $0.112$  rad, two anti-Stokes rings were observed; the more intense ring corresponding to a cone angle of  $0.11$  rad (with Stokes along the axis) and the weaker ring corresponding to the angle  $0.15$  rad (with Stokes slightly off the axis and laser radiation at the periphery of the beam). These results are shown in Fig. 6, and confirm the above explanation.

Further confirmation is found in the dependence of the second-order Stokes emission angle on convergence of the laser beam

shown in Fig. 3. From the wave-vector diagram in Fig. 5(b), it is seen that with increasing angle of the laser radiation, first-order Stokes radiation closer to the axis is effective in producing second-order Stokes emission. Moreover, the emission angle decreases with increasing angle of convergence of laser radiation. It reaches the limiting value  $0.116 - 0.043$ , or  $0.07$  rad (see Table I) with Stokes radiation on axis. This explains the behaviour shown in Fig. 3.

It is also evident from the above explanation of the importance of beam convergence that when a cylindrical lens (or a long slit) is used to focus the laser beam the "ring" patterns (Fig. 1) will be replaced by "elliptical patterns", the minor axis being determined by the cylinder axis (or length of slit). Moreover, maxima of intensity will occur at the extremities of the major axis, since the gain would be largest for Stokes radiation closest to the beam axis. "Elliptical" patterns exhibiting these features have been observed with calcite<sup>4</sup> and with Class I radiation from various liquids<sup>5</sup> and now with diamond. An example is shown in Fig. 7.

#### F. Conclusion

The present investigation of the angular distribution of stimulated Raman radiation in diamond confirms the earlier results obtained with calcite (Chiao and Stoicheff<sup>4</sup>) and considerably extends our knowledge of the production of Class I radiation in solids. The observed angular distribution and its dependence on the angle of convergence of the incident laser beam finds a ready explanation in the available theory, especially as formulated by Garmire, Pandarese and Townes<sup>1</sup>.



### References

1. E. Garmire, F. Pandarese, C.H. Townes, Phys. Rev. Letters 11, 160 (1963).
2. N. Bloembergen and Y.R. Shen, Phys. Rev. Letters 12, 504 (1964).
3. P.D. Maker and R.W. Terhune, Phys. Rev. 137, A801 (1965).
4. R.Y. Chiao and B.P. Stoicheff, Phys. Rev. Letters 12, 290 (1964).
5. E. Garmire, Phys. Letters 17, 251 (1965); in Physics of Quantum Electronics (eds. P.L. Kelley, E. Lax and P.E. Tannenwold) McGraw-Hill, New York, p. 167 (1966).
6. G. Eckhardt, D.P. Bortfeld and M. Geller, App. Phys. Letters, 3, 137 (1963).

Table 1

DIAMOND				
Frequency	Emission Expt.	Angles Theory	Absorption Expt.	Angles Theory
$\omega_0 - 2\omega_r$	0.116	0.119	(0.048)	0.043
$\omega_0 + \omega_r$	.053	.053	.060	.064
$\omega_0 + 2\omega_r$	.103	.104	(.079)	.071
$\omega_0 + 3\omega_r$	.158	.152	----	.079

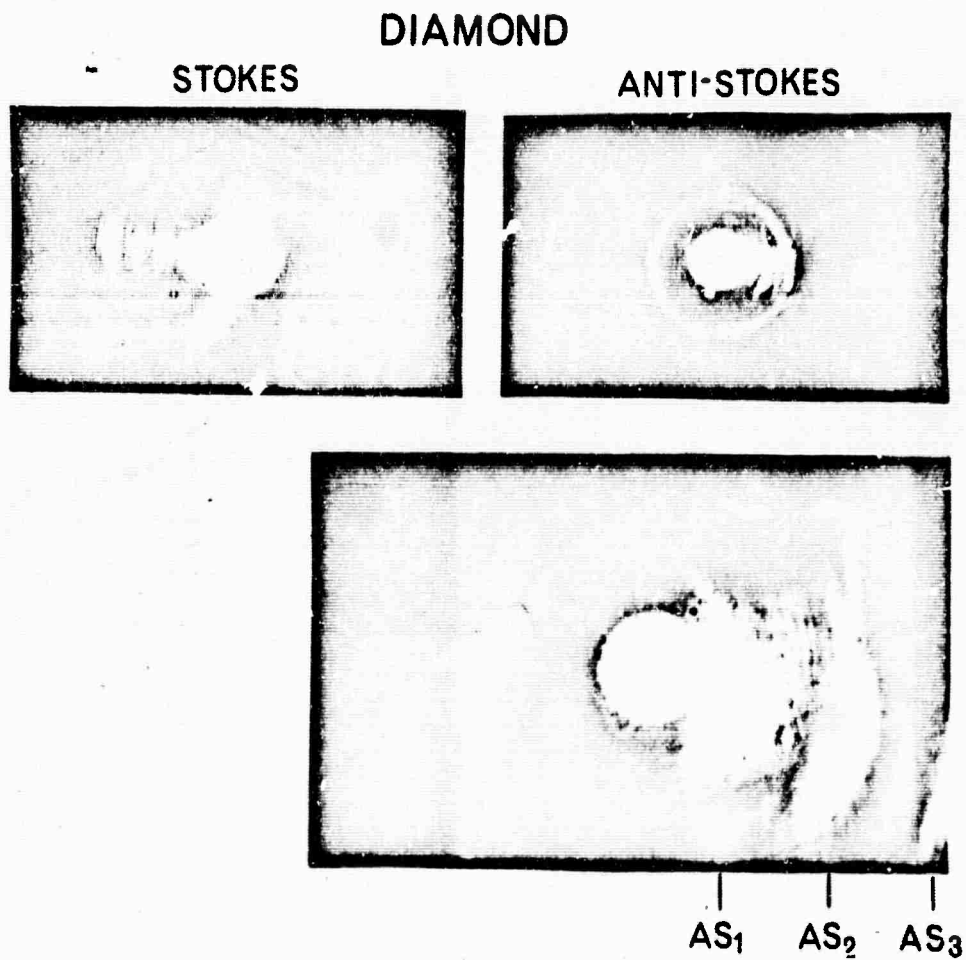


Fig. 1.

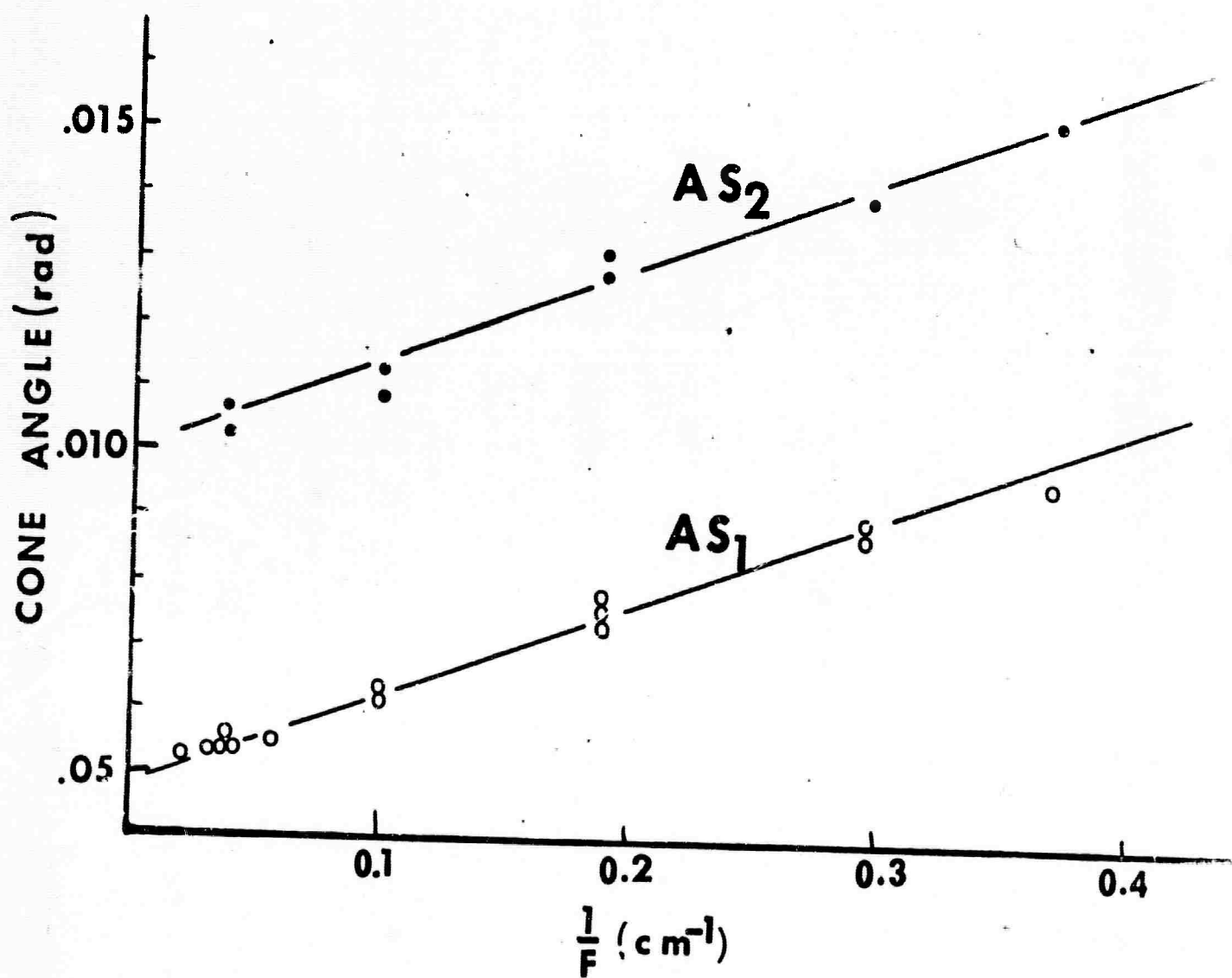


Fig. 2

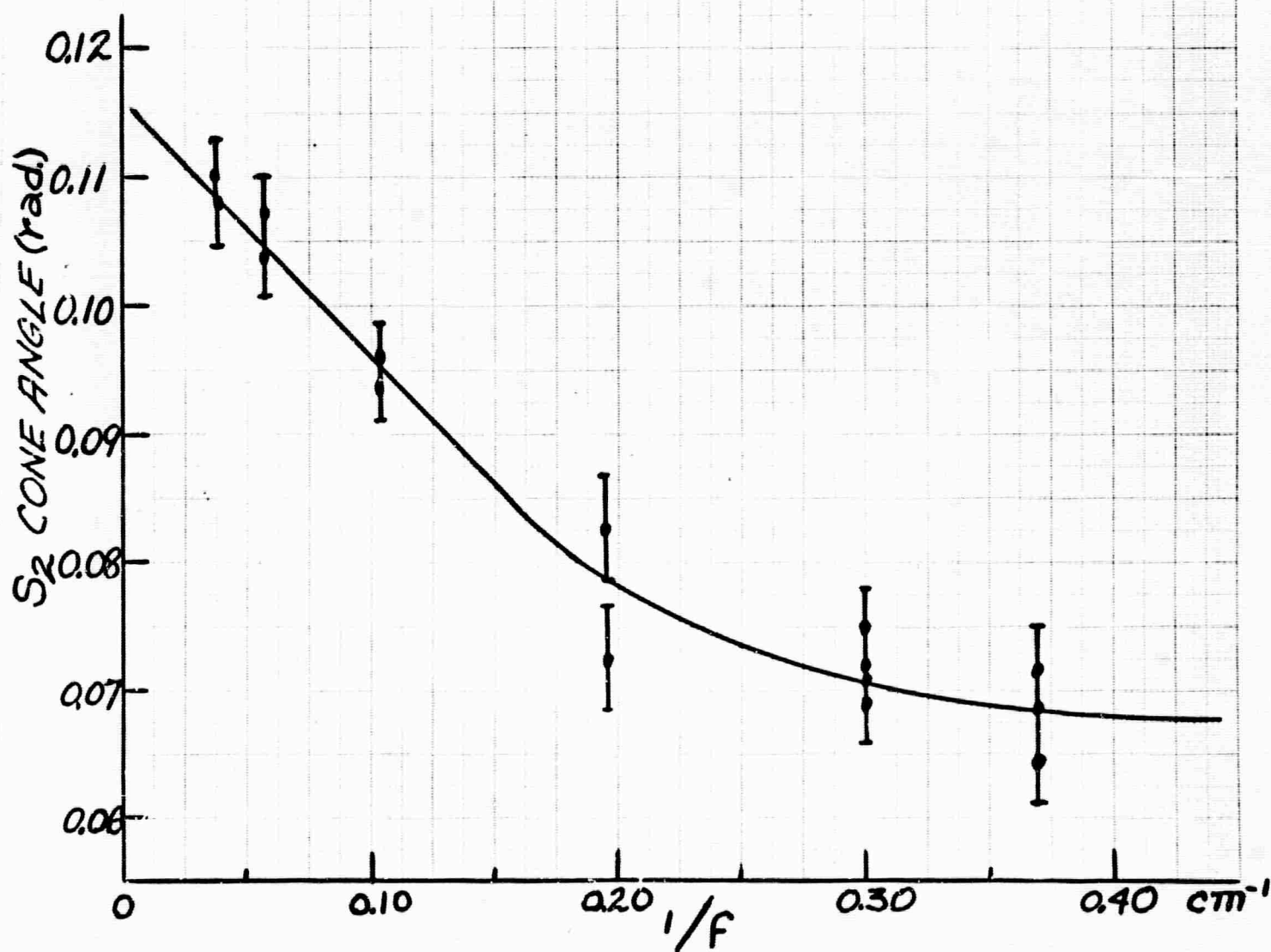


Fig. 3

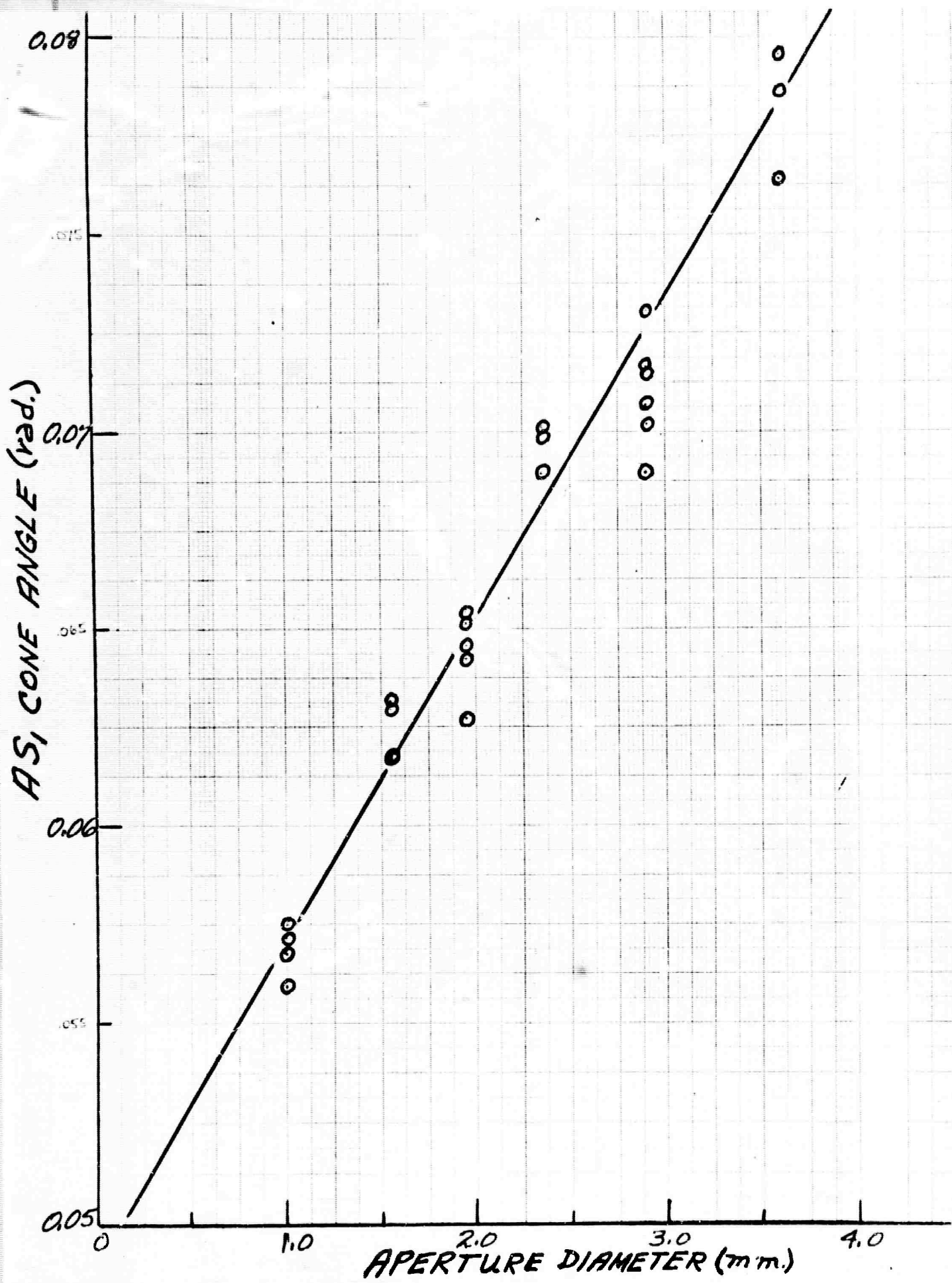
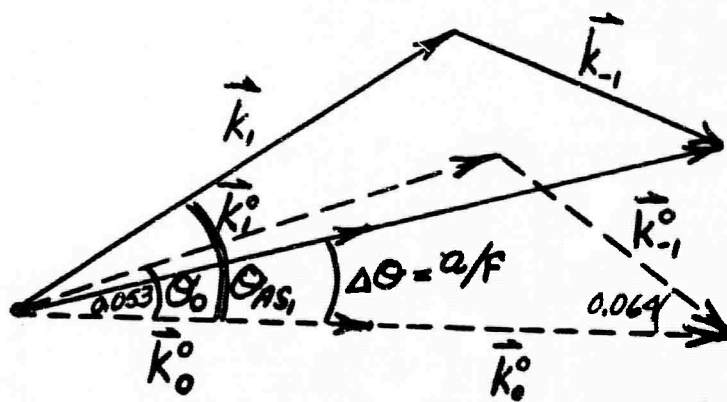
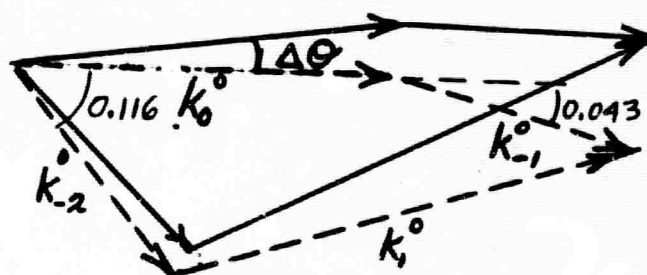


Fig. 4



(a)



(b)

Fig 5.



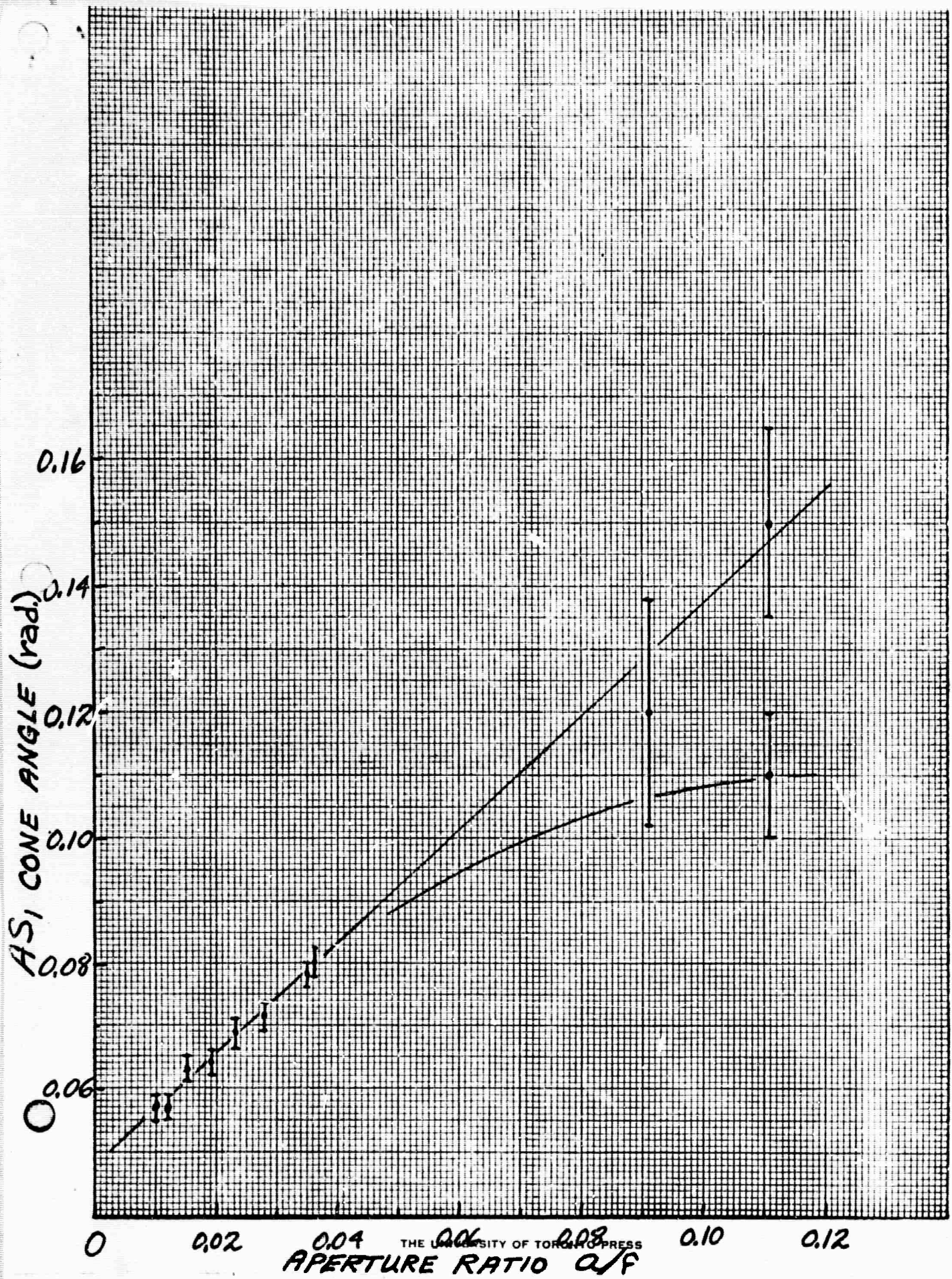
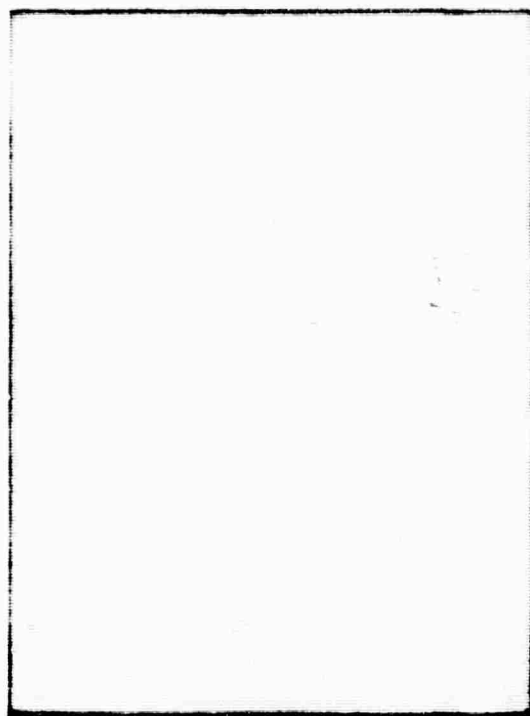


Fig. 6.



CYLINDRICAL  
LENS AXIS



Fig. 7



# Generation of "Surface" Radiation in Stimulated Raman Scattering from Liquid Mixtures

F. Shimizu, U. Bachmann and B.P. Stoicheff

The emission of anti-Stokes radiation during the stimulated Raman process is known to have specific directional distributions which are strongly dependent on the experimental conditions. The two commonly observed distributions have been labelled Class I and II by Garmire<sup>1</sup> (1965). Class I distribution is given by the momentum-matching condition for plane waves,  $k_0 + k_{n-1} = k_{-1} + k_n$  where the anti-Stokes radiation of the  $n$ th order  $k_n$  is generated from the laser  $k_0$ , the first order Stokes  $k_{-1}$  and the  $(n-1)$  order radiation. Such distribution of anti-Stokes radiation has been observed in calcite<sup>2</sup> (Chiao and Stoicheff, 1964) in diamond<sup>3</sup> (McQuillan and Stoicheff) and in several liquids where feedback of Stokes radiation at the phase-matching angle is present<sup>1</sup>. Class II distribution occurs at larger angles than Class I and has been observed in liquids only. The relevant process is not understood.

A distribution of anti-Stokes emission which is different from Class I and II has been proposed by Szoke<sup>4</sup> (1964) and labelled "surface" radiation. It is characterized by the relation

$$k_1 \cos \theta = 2 k_0 - k_{-1} \quad (1)$$

and may occur when first order Stokes radiation is strongly directional and parallel to the incident laser wave. Maker and Terhune<sup>5</sup> (1965) have observed radiation which approaches this

distribution in the limit that the longitudinal but not the transverse components of the phase velocities sum to zero. More recently Shimoda<sup>6</sup> (1966) has presented a comprehensive account of the angular distribution and shown that "surface" radiation may occur in the presence of first Stokes radiation in filaments which are very long in comparison with their diameter.

We report here the observation of "surface" radiation in acetone and in cyclohexane under experimental conditions which satisfy the boundary conditions of the theory. We have observed first-order anti-Stokes emission in sharply-defined cones in the forward direction having precisely the angle  $\theta$  given by Eq. (1). At the same time first-order Stokes radiation has been observed in very fine filaments produced by self-trapping of the radiation.

In pure acetone and pure cyclohexane, usually, only the Class I distribution of anti-Stokes radiation is produced. Examples of this distribution as excited by a giant-pulse ruby laser are shown in Fig. 1(a) and Fig. 2(a). The corresponding wave vector diagram is given in Fig. 3(a). When a small amount (5 to 10%) of carbon disulphide is added to acetone or to cyclohexane the angular distribution is completely different. It usually consists of sharp rings as shown in Fig. 1(b) and Fig. 2(b) which correspond to the "surface" radiation. On occasion the Class II rings are observed in addition to the much sharper "surface" rings (cf. Fig. 1(b) and Fig. 2(b)). The cone angles for all three distributions are given in Table I. The

threshold for appearance of "surface" radiation appears to be the same as for Class I and II radiation. Finally, it should be emphasized that only stimulated Raman radiation from acetone or cyclohexane, corresponding to the C-H vibration at about  $2900\text{ cm}^{-1}$ , was observed in these experiments and none which could be attributed to carbon disulphide.

The observation of "surface" radiation under our experimental conditions finds a ready explanation in the fact that carbon disulphide is one of the strongest self-focussing liquids<sup>7</sup> (Chiao, Garmire and Townes, 1964). Thus the laser beam is self-focussed and trapped in one or more fine filaments producing very high electric fields within the filaments. These fields are surely sufficient to produce Stokes radiation in the filaments, both in the forward and backward direction; the interaction of this Stokes radiation with laser radiation then gives rise to anti-Stokes radiation with the angular distribution shown in the wave-vector diagram of Fig. 3(b) and given by Eq. (1). Photographs of the exit end of the sample cell taken at a magnification of 20 confirmed that first Stokes radiation is produced in one or more filaments having diameters of approximately 10-20 micron. Each filament produced its own sharp and separate ring.

The present observations of surface radiation confirm the predictions of Szoke and Shimoda. The simple model which most adequately represents the conditions of observation is that of a linear array of radiating dipoles. The resultant radiation

pattern is that of the familiar dipole antenna and is represented by Eq. (1).

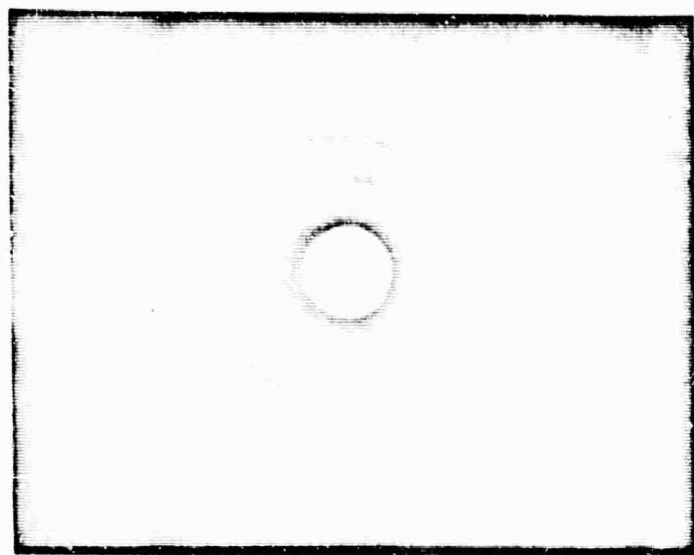
References

1. E. Garmire, Phys. Letters 17, 251 (1965).
2. R.Y. Chiao and B.P. Stoicheff, Phys. Rev. Letters 12, 290 (1964).
3. A.K. McQuillan and B.P. Stoicheff, unpublished (see Report I).
4. A. Szoke, Bull. Am. Phys. Soc. 9, 490 (1964).
5. P.D. Maker and R.W. Terhune, Phys. Rev. 137, A 801 (1965).
6. K. Shimoda, Japan J. Appl. Phys. 5, 86 (1966).
7. R.Y. Chiao, E. Garmire and C.H. Townes, Phys. Rev. Letters 13, 479 (1964).

Table I

Cone Angles (in radians) for Anti-Stokes Emission

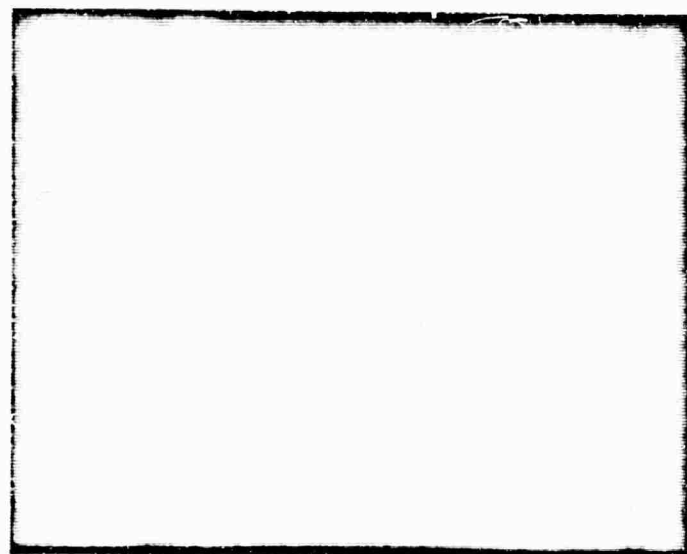
<u>Distribution</u>	<u>Acetone</u>		<u>Cyclohexane</u>	
	<u>Calc.</u>	<u>Obs.</u>	<u>Calc.</u>	<u>Obs.</u>
Class I	0.040	$0.040 \pm 0.002$	0.043	$0.043 \pm 0.002$
Class II		$0.057 \pm 0.002$		$0.052 \pm 0.002$
Surface	0.063	$0.063 \pm 0.001$	0.068	$0.068 \pm 0.001$



(a) Class I

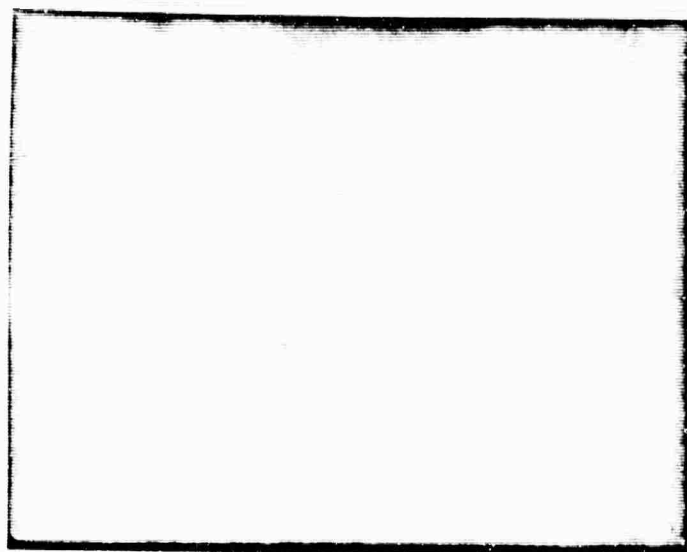


(b) Class II

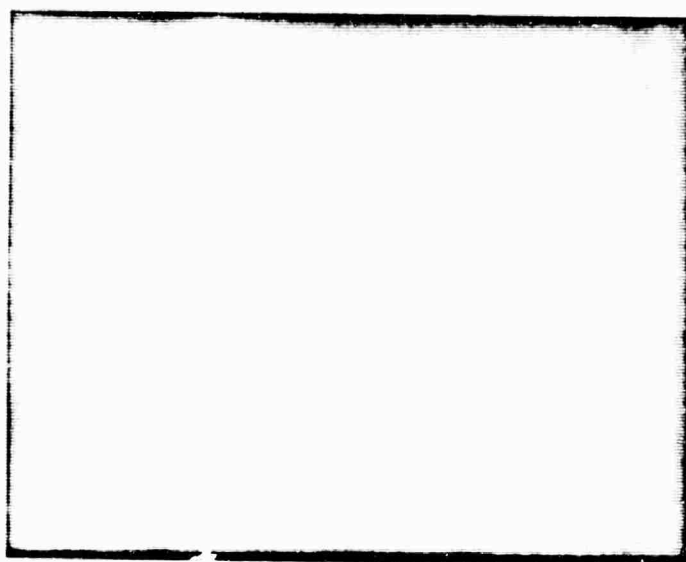


(c) Surface

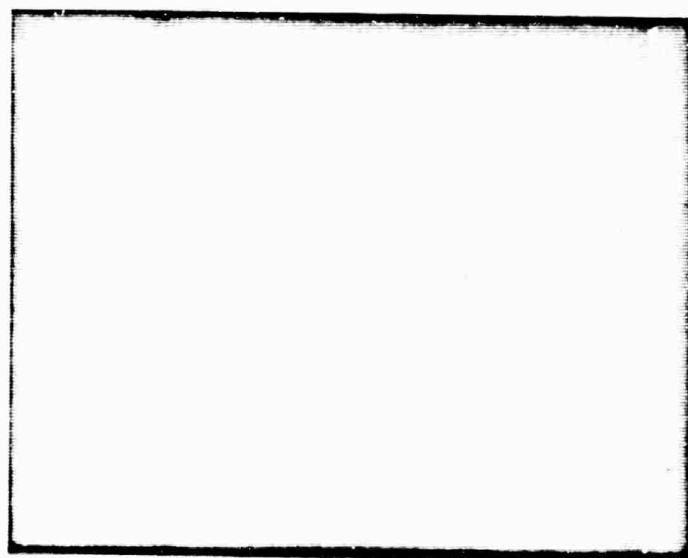
Fig.1. Angular distribution of anti-Stokes radiation in acetone.  
(a) pure acetone, (b) and (c) mixture of acetone and  
8 percent carbon disulphide.



(a) Class I



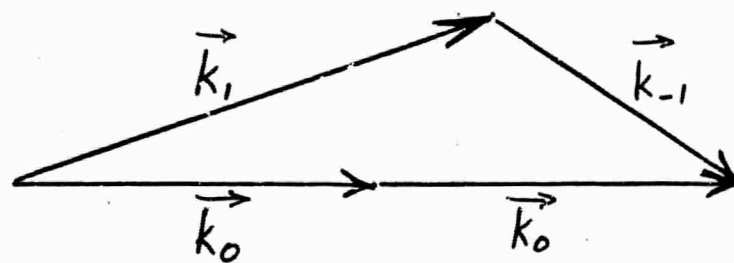
(b) Class II



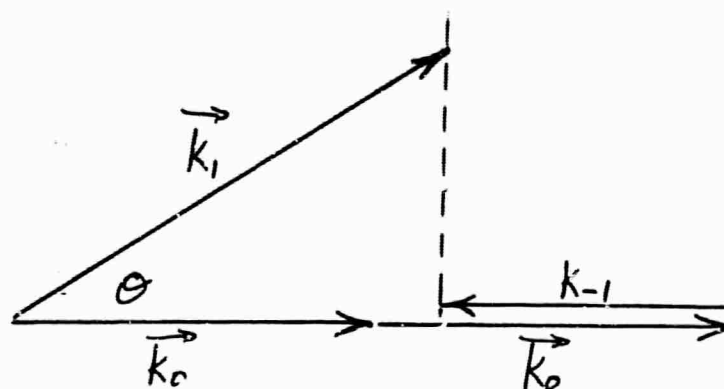
(c) Surface

Fig.2. Angular distribution of anti-Stokes radiation in cyclohexane.  
(a) and (b) pure cyclohexane, (c) mixture of cyclohexane and  
5 percent carbon disulphide.





(a)



(b)

Fig.3. Wave vector diagrams for Class I (a) and "Surface" (b) radiation.

## Line Width Measurements in Raman Spectroscopy

W. Clements and B.P. Stoicheff

From the earliest observations of Raman spectra it has been known that Raman bands corresponding to the totally symmetric vibrations of molecules exhibit extremely sharp lines, not only in gases but also in liquids and solids. Until recently, very few studies of the Raman effect have been concerned with line width measurements, with the exception of some studies of pressure broadening in  $H_2$ ,  $O_2$ , and  $N_2$ . With the discovery of the stimulated Raman scattering there has been a need for such measurements since the threshold for stimulated scattering is inversely proportional to the line width. Several approximate measurements for liquids have been reported in the recent literature. However, the most accurate measurement is perhaps that of Parks<sup>1</sup> who recently measured a width of  $1.14 \pm 0.08 \text{ cm}^{-1}$  for the  $1086 \text{ cm}^{-1}$  vibrational band of calcite. He excited the spectrum with a He-Ne laser and used a grating spectrometer with photoelectric detection. In the present paper we describe an apparatus for Raman line width measurements using a narrow exciting line from a powerful He-Ne laser together with a high-resolution, pressure-scanned Fabry-Perot interferometer. With this apparatus we have measured the full width at half intensity of liquid  $CS_2$  and found it to be  $0.47 \pm 0.05 \text{ cm}^{-1}$ .

### Apparatus

The apparatus and technique will be described with the aid of Fig. 1. The He-Ne laser was built in this laboratory. It is a design using a large diameter (15 mm.) tube, so that the gain is

low, leading to a relatively narrow emission line. By making the laser 4 m. in length reasonable output power at 6328 was achieved. With output power of 250 mW a line width of 750 Mc/sec or  $0.025 \text{ cm}^{-1}$  was obtained. (It may be noted that this width is approximately 10 per cent of the widths of the 4880 Å or 5145 Å lines from  $\text{Ar}^+$  laser.) Such a line width is ideal for almost any Raman linewidth measurement including heavy gases since typical Doppler breadths are of the order of  $0.05 \text{ cm}^{-1}$ . The  $\lambda 6328$  line from the laser was isolated by an interference filter, focussed on to a small mirror (2 mm diameter) on a glass plate and reflected into a 3 mm diameter capillary tube which served as the liquid sample cell. The capillary walls acted as a light guide for the exciting light and for the Raman scattered light observed at about  $10^\circ$  to the incident direction. This Raman light was passed through an interference filter which suppressed the laser light, and then collected by a large diameter lens and transmitted through a Fabry-Perot interferometer. A camera lens focussed the interference rings on a screen. A small aperture was centred on the ring pattern and behind it was placed a sensitive photomultiplier. The spectrum was scanned over a very small spectral range by changing the gas pressure in the F.P. interferometer: In effect this varies the optical path length which can be controlled in a linear way by a linear pressure variation. This leads to a repetition of the spectrum (sometimes called a "stick-spectrum") with spacing  $c/2l$  where  $c$  is the velocity of light and  $l$  the interferometer spacing. In our apparatus, with a spacing of 3 mm, the free spectral range is  $5 \times 10^9 \text{ cps}$  or  $1.6 \text{ cm}^{-1}$

as shown in the sample spectrum in Fig. 2. The interferometer reflectivity is 98%, resulting in a resolving power  $\lambda/\Delta\lambda$  (or  $\nu/\Delta\nu$ ) greater than  $10^6$ . The practical resolving power, however, is limited to  $6 \times 10^5$  because of the  $0.025 \text{ cm}^{-1}$  linewidth of the  $6328 \text{ \AA}$  line.

#### Line Width of Liquid $\text{CS}_2$

One of the strongest known Raman lines is the  $656 \text{ cm}^{-1}$  line of liquid  $\text{CS}_2$ . It appears to have the lowest threshold for stimulated scattering and produces very strong self-focusing. An interferogram of the  $656 \text{ cm}^{-1}$  line is shown in Fig. 2 in which three adjacent orders are displayed having separations of  $1.60 \text{ cm}^{-1}$ . Measurements of the half width (full width at half intensity) give the surprising result of  $\Delta\nu_{\frac{1}{2}} = 0.47 \pm 0.05 \text{ cm}^{-1}$ . This is to be compared with the value of  $1.0 \text{ cm}^{-1}$  measured by Stoicheff<sup>2</sup>, and the earlier value of  $3.0 \text{ cm}^{-1}$  which has been used in almost all recent calculations of the Raman gain in  $\text{CS}_2$ <sup>3,4</sup>. Thus, for example, Garmire<sup>3</sup> and Bisson, Bret et al<sup>4</sup> have calculated a value of approximately 60 for the gain in  $\text{CS}_2$ . From our measurements of the line width this value should be increased by the factor  $3.0/0.47$  or about 6, leading to a gain of 360 for  $\text{CS}_2$ .

#### Conclusion

Clearly, the accurate measurement of line widths in the normal Raman effect are important if we are to understand the gain problem in the stimulated scattering. Other liquids are now under study, as well as solids such as diamond and calcite.

## References

1. K. Park, Physics Letters 22, 39 (1966).
2. B.P. Stoicheff, Physics Letters 7, 186 (1963).
3. E. Garmire, Thesis, M.I.T. (1965).
4. G. Bisson, G. Bret, M. Denariez, F. Gires, G. Mayer et M. Paillette, J. de Chimie Physique 64, 197 (1967).

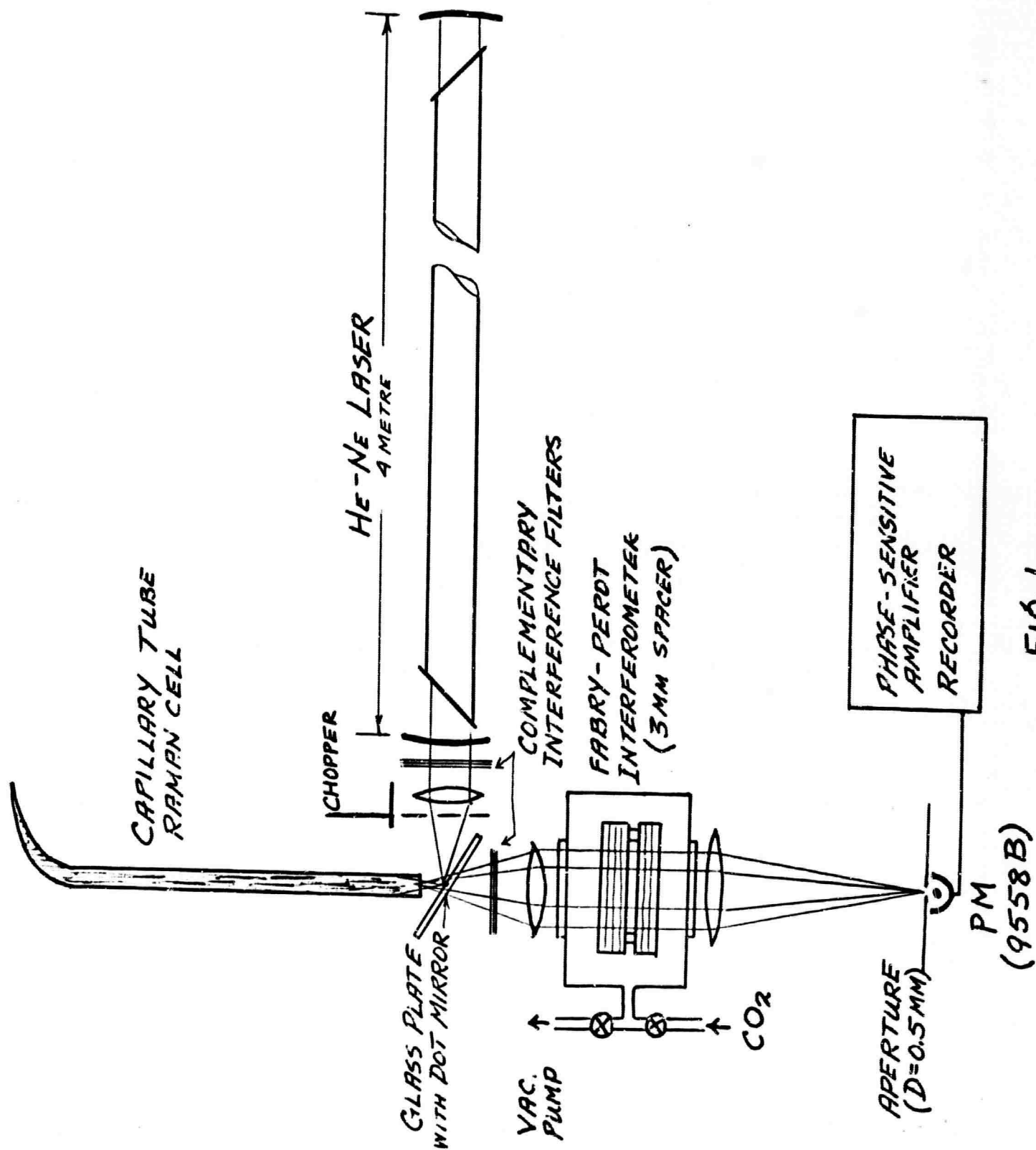
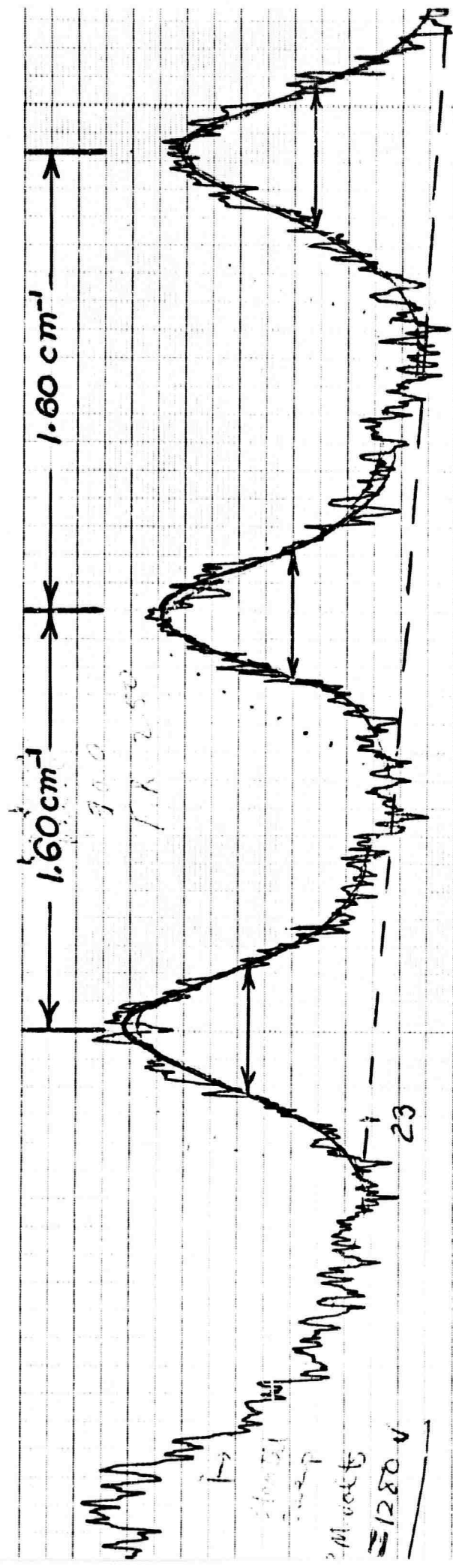


Fig. 1.



LIQUID CS<sub>2</sub>

$\nu_R = 655.6 \text{ cm}^{-1}$

Fig. 2

## Security Classification

## DOCUMENT CONTROL DATA - R&amp;D

(Security classification of title, body of abstract and indexing annotation must be entered when the overall report is classified)

## 1. ORIGINATING ACTIVITY (Corporate author)

Department of Physics  
University of Toronto  
Toronto 5, Ontario.

## 2a. REPORT SECURITY CLASSIFICATION

Unclassified

## 2b. GROUP

## 3. REPORT TITLE

Normal and Stimulated Raman Spectroscopy

## 4. DESCRIPTIVE NOTES (Type of report and inclusive dates)

Semi Annual Reports No. 1 1 June 1965 - 31 Dec. 1965  
No. 2 1 Jan. 1966 - 31 May 1966  
No. 3 1 June 1966 - 31 Dec. 1966

## 5. AUTHOR(S) (Last name, first name, initial)

Stoicheff, Boris P. Clements, W.  
Shimizu, F. Bachmann, U.  
McQuillan, A.K.

## 6. REPORT DATE

April 1967

## 7a. TOTAL NO. OF PAGES

30

## 7b. NO. OF REFS

17

## 8a. CONTRACT OR GRANT NO.

Nonr-5012(00)

## b. PROJECT NO.

c. NR 015-813/4-14-65

## 8b. ORIGINATOR'S REPORT NUMBER(S)

Semi-Annual Reports  
No. 1, No. 2, No. 3

## 8c. OTHER REPORT NO(S) (Any other numbers that may be assigned this report)

d. Authorization ARPA Order No. 306

## 10. AVAILABILITY/LIMITATION NOTICES

Distribution of this document is unlimited.

## 11. SUPPLEMENTARY NOTES

## 12. SPONSORING MILITARY ACTIVITY

Office of Naval Research and  
Advanced Research Projects Agency

## 13. ABSTRACT

This report is in three parts:

Part 1 gives a detailed account of experiments on the angular dependence of stimulated Raman emission in diamond. The observed cone angles of Stokes and anti-Stokes radiation produced by incident parallel light agree with the momentum-matching condition for plane waves. Furthermore, it was found that the cone angles were independent of laser intensity, but sensitively dependent on the angle of convergence of the incident laser radiation. These observations are explained on the basis of the available theory of the stimulated Raman process.

Part 2 reports on first observation of so-called "surface" radiation in stimulated Raman scattering. In pure acetone and cyclohexane, usually Class I radiation is observed. In mixtures with 5 to 10%  $\text{CS}_2$  we have observed first-order anti-Stokes emission (at  $\nu_R = 2920 \text{ cm}^{-1}$  for acetone and  $2850 \text{ cm}^{-1}$  for cyclohexane) in sharply defined cones which obey the wave-vector relation  $k_1 \cos \theta = 2k_0 - k_1$ . This implies that only the longitudinal and not the transverse components of the phase velocities sum to zero.

Part 3 describes a technique, using a He-Ne laser of 250 mW output and 750 Mc/sec (or  $0.025 \text{ cm}^{-1}$ ) line width, for measuring "spontaneous" Raman line widths. The  $656 \text{ cm}^{-1}$  band of liquid  $\text{CS}_2$  was found to have a line width of  $0.47 \pm 0.05 \text{ cm}^{-1}$ . This yields for the calculated gain in the stimulated emission a value of 360 rather than the earlier value



14. KEY WORDS	LINK A		LINK B		LINK C	
	ROLE	WT	ROLE	WT	ROLE	WT
Stimulated Raman Emission Angular Distribution of Stimulated Raman Scattering Generation of "Surface" Radiation in Stimulated Raman Scattering Raman Line Widths						

RECEI  
JUL 21 1967  
CFSTI

## INSTRUCTIONS

1. **ORIGINATING ACTIVITY:** Enter the name and address of the contractor, subcontractor, grantee, Department of Defense activity or other organization (corporate author) issuing the report.

2a. **REPORT SECURITY CLASSIFICATION:** Enter the overall security classification of the report. Indicate whether "Restricted Data" is included. Marking is to be in accordance with appropriate security regulations.

2b. **GROUP:** Automatic downgrading is specified in DoD Directive 5200.10 and Armed Forces Industrial Manual. Enter the group number. Also, when applicable, show that optional markings have been used for Group 3 and Group 4 as authorized.

3. **REPORT TITLE:** Enter the complete report title in all capital letters. Titles in all cases should be unclassified. If a meaningful title cannot be selected without classification, show title classification in all capitals in parenthesis immediately following the title.

4. **DESCRIPTIVE NOTES:** If appropriate, enter the type of report, e.g., interim, progress, summary, annual, or final. Give the inclusive dates when a specific reporting period is covered.

5. **AUTHOR(S):** Enter the name(s) of author(s) as shown on or in the report. Enter last name, first name, middle initial. If military, show rank and branch of service. The name of the principal author is an absolute minimum requirement.

6. **REPORT DATE:** Enter the date of the report as day, month, year, or month, year. If more than one date appears on the report, use date of publication.

7a. **TOTAL NUMBER OF PAGES:** The total page count should follow normal pagination procedures, i.e., enter the number of pages containing information.

7b. **NUMBER OF REFERENCES:** Enter the total number of references cited in the report.

8a. **CONTRACT OR GRANT NUMBER:** If appropriate, enter the applicable number of the contract or grant under which the report was written.

8b, 8c, & 8d. **PROJECT NUMBER:** Enter the appropriate military department identification, such as project number, subproject number, system numbers, task number, etc.

9a. **ORIGINATOR'S REPORT NUMBER(S):** Enter the official report number by which the document will be identified and controlled by the originating activity. This number must be unique to this report.

9b. **OTHER REPORT NUMBER(S):** If the report has been assigned any other report numbers (either by the originator or by the sponsor), also enter this number(s).

10. **AVAILABILITY/LIMITATION NOTICES:** Enter any limitations on further dissemination of the report, other than those

imposed by security classification, using standard statements such as:

- (1) "Qualified requesters may obtain copies of this report from DDC."
- (2) "Foreign announcement and dissemination of this report by DDC is not authorized."
- (3) "U. S. Government agencies may obtain copies of this report directly from DDC. Other qualified DDC users shall request through \_\_\_\_\_."
- (4) "U. S. military agencies may obtain copies of this report directly from DDC. Other qualified users shall request through \_\_\_\_\_."
- (5) "All distribution of this report is controlled. Qualified DDC users shall request through \_\_\_\_\_."

If the report has been furnished to the Office of Technical Services, Department of Commerce, for sale to the public, indicate this fact and enter the price, if known.

11. **SUPPLEMENTARY NOTES:** Use for additional explanatory notes.

12. **SPONSORING MILITARY ACTIVITY:** Enter the name of the departmental project office or laboratory sponsoring (paying for) the research and development. Include address.

13. **ABSTRACT:** Enter an abstract giving a brief and factual summary of the document indicative of the report, even though it may also appear elsewhere in the body of the technical report. If additional space is required, a continuation sheet shall be attached.

It is highly desirable that the abstract of classified reports be unclassified. Each paragraph of the abstract shall end with an indication of the military security classification of the information in the paragraph, represented as (TS), (S), (C), or (U).

There is no limitation on the length of the abstract. However, the suggested length is from 150 to 225 words.

14. **KEY WORDS:** Key words are technically meaningful terms or short phrases that characterize a report and may be used as index entries for cataloging the report. Key words must be selected so that no security classification is required. Identifiers, such as equipment model designation, trade name, military project code name, geographic location, may be used as key words but will be followed by an indication of technical context. The assignment of links, roles, and weights is optional.